Simulation of the heating up of the propellant charge body of a high precision machine gun during firing

Dr. Manfred A. Bohn*) and Dr. Axel Pfersmann**)

*) Fraunhofer ICT, Pfinztal, Germany

**) Diehl BGT Defence, Roethenbach a.d. Pegnitz, Germany

Presentation on the

8th International Heat Flow Calorimetry Symposium on Energetic Materials (HFC-S EM)

October 29 – 31, 2012

Wokefield Park, Mortimer

Reading, West Berkshire, UK

Heat Flow Calorimetry

International

HFCS-EM

Symposium

on Energetic Materials

Fraunhofer ICT

DIEHL BGT Defence

Motivations and Objectives

- Company Diehl introduced a new concept of the ammunition loading for a machine gun
- Separate loading of the projectile and the caseless propellant body
- Company Diehl asked ICT for support to protect the charge body against thermal threats

- Development of a thermal insulation for the charge body based on hard energetic PUR foam
- Estimation of time to ignition of the propellant body if placed in a hot burning chamber

Visualization of the two chambers and view on the caseless propellant body

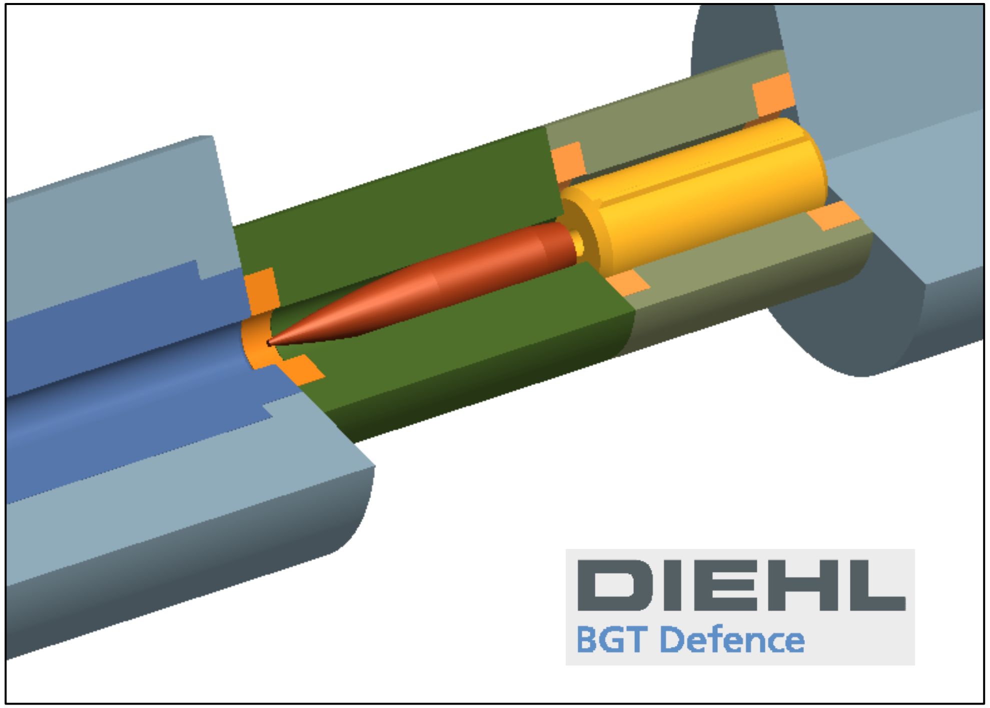

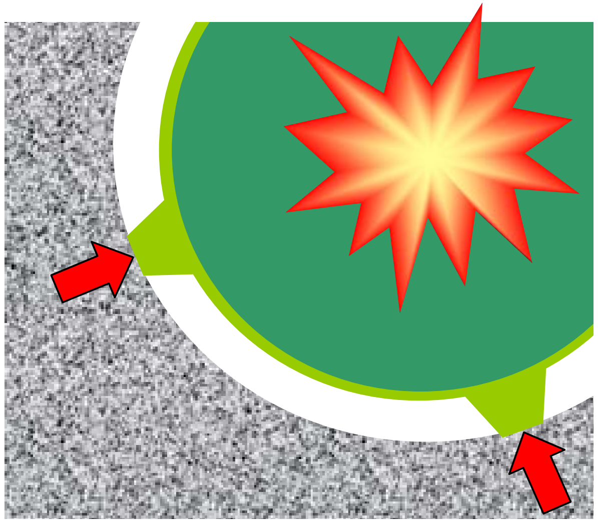

New concept of a high precision machine gun, 12.7mm
Uses separated loading of projectile and caseless charge

Caseless charge is a consolidated body made from glued ball powder
Thermally insulated by PUR foam with 50 mass-% HMX by a coating of the body and by four spacers

The caseless propellant body

The propellant body is a cylindrical body made of glued double base ball powder (AkII stabilized) containing nitroglycerine.

For protection against direct flame ignition it has a coating.

Further four spacers have been applied in 90° distance on the outside

The coating and the spacers are made of hard polyurethane foam filled with 50 mass-% HMX

The foam and its application have been worked out at Fraunhofer ICT in the group of Dr. Böhnlein-Mauß

Principle functioning of the machine gun - 1

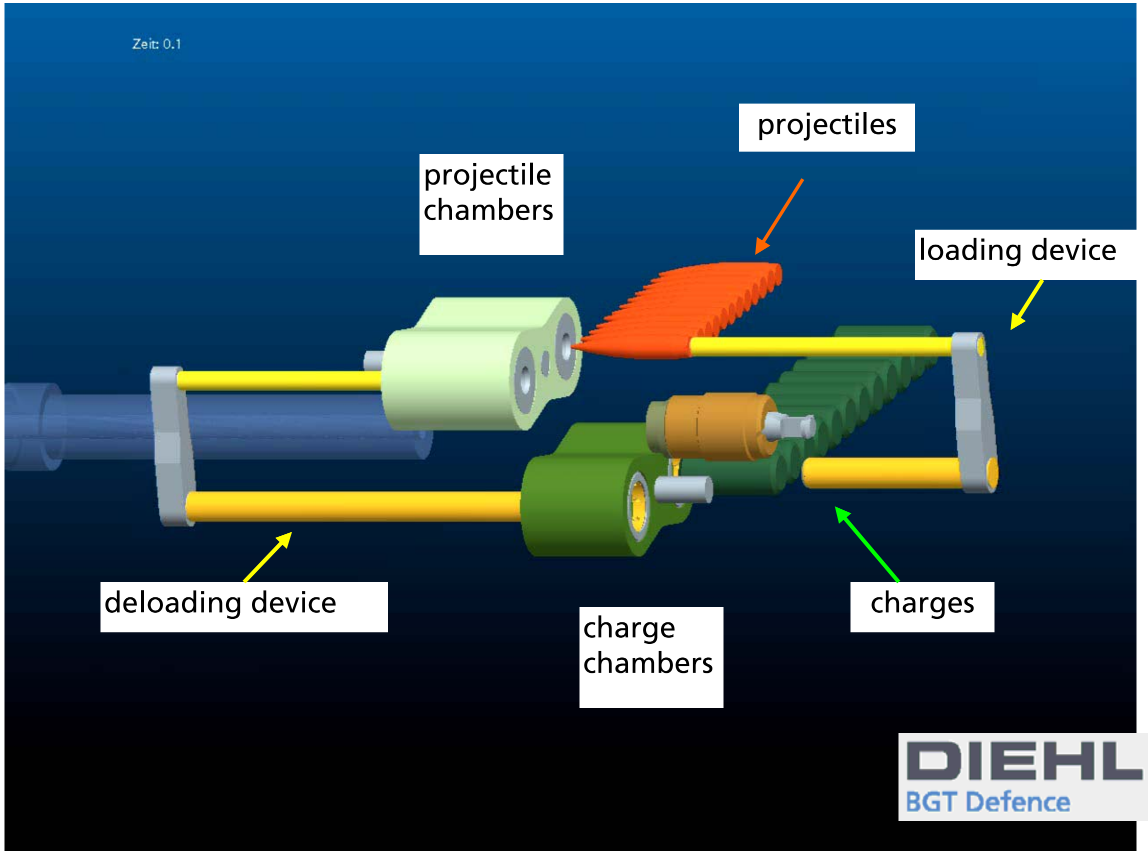

Start position, just before loading cycle

Above the double projectile chamber, below the double charge chamber

Principle functioning of the machine gun - 2

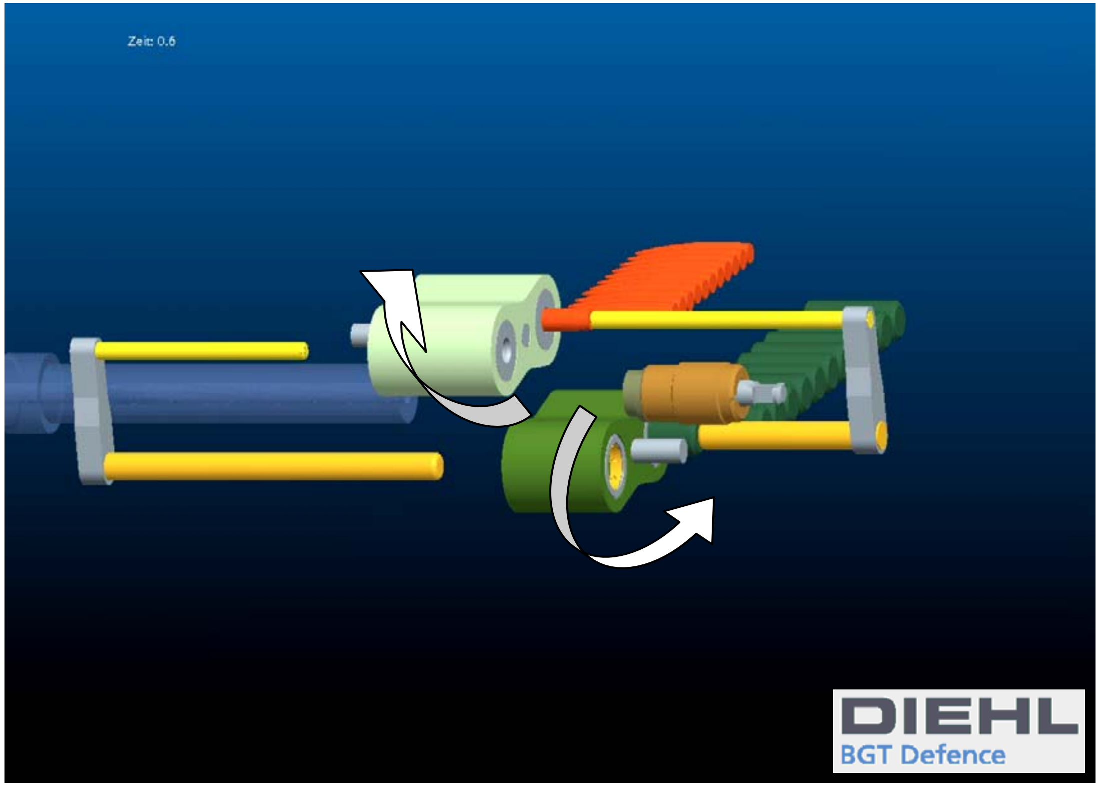

Loading the projectile (above) and the charge (below) simultaneously in the two different chambers.

After the loading, the two double chambers counter rotate by 90° into the firing position, where loaded projectile chamber and loaded charge chamber are in line

Principle functioning of the machine gun - 3

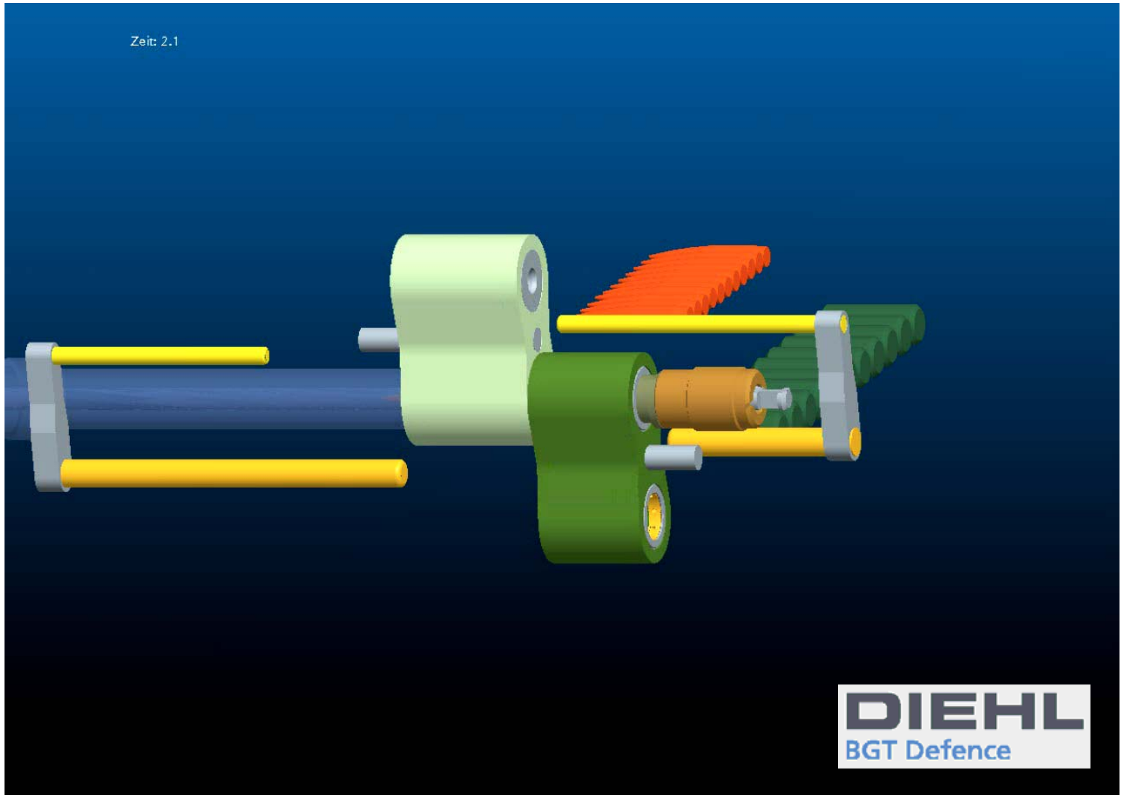

Firing position,

the breech of the charge chamber is closed.

After firing, the two double chambers counter rotate further by 90° back to the deloading and loading position.

Principle functioning of the machine gun - 4

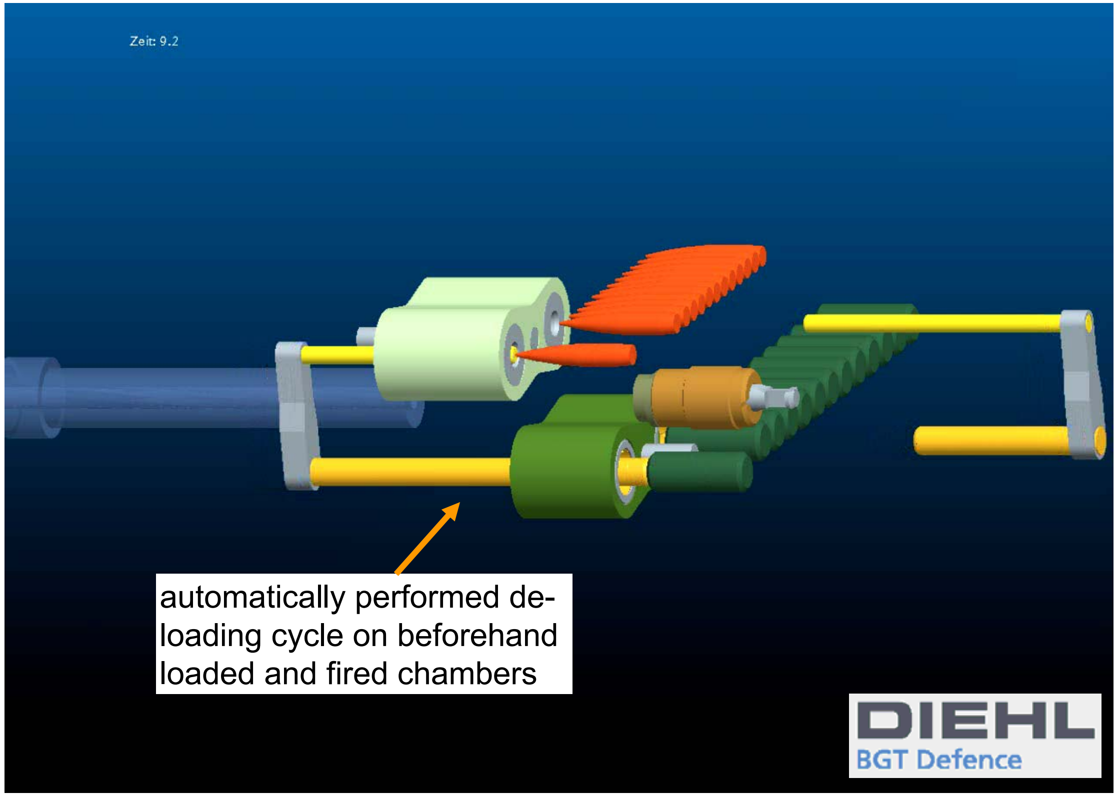

Before loading again, the two chambers from the beforehand firing position are checked by the deloading device.

If the shot would have been unsuccessful, these chambers will be cleared before their next loading.

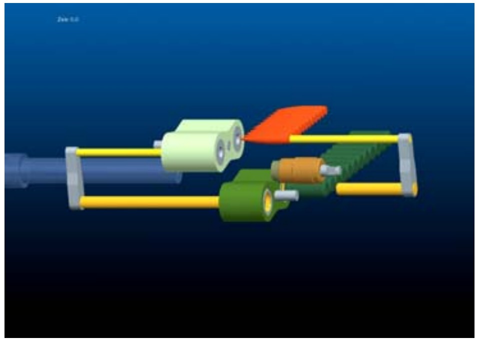

Simulation of the cook-off behaviour of PUR foam spacer, PUR foam coating and propellant body PB

General heat balance equation and special cases

$$c_P \cdot \rho \cdot \frac{dT(t,\vec{r})}{dt} = \rho \cdot \frac{dQ\ (T(t,\vec{r}))}{dt} + \mathrm{div}\left(\lambda \cdot \mathrm{grad}\,T(t,\vec{r})\right) - \frac{h \cdot S}{V}\left(T(t,\vec{r}) - Tw\right)$$

temp. change of the sample	heat generation in the sample	heat conduction in the sample	heat transfer between sample and environment

$$\rho \cdot \frac{dQ\ (T(t,\vec{r}))}{dt} = -\,\mathrm{div}\left(\lambda \cdot \mathrm{grad}\,T(t,\vec{r})\right)$$

Heat generation equals heat conduction in material

Frank-Kamenetzkii (FK case)

To be used for solids with low to medium heat conductivity
Approximative for unstirred liquids and gases
!! Assumes infinite fast heat transfer at the outside of body to the environment !!

$$\rho \cdot \frac{dQ\ (T(t,\vec{r}))}{dt} = \frac{h \cdot S}{V}\left(T(t,\vec{r}) - Tw\right)$$

Heat generation equals heat transfer to environment

Semenov (Se case)

To be used for well stirred reaction vessel,
equal temperature inside the liquid material

Both special cases consider only the stationary situation (means dependence from space only),

no time dependence, no influence of consumption of material

Frank-Kamenetzkii evaluation - improved expression

Boundary condition: $\lambda\left(\frac{dT}{dr}\right)\Big|_{r=r_0} = -h\cdot(T_S - Tw)$

$$\frac{1}{\delta c_v} = \frac{1}{\delta c_c} + 2\cdot e\cdot\frac{\lambda}{2\cdot r_0\cdot h}\cdot\frac{V}{S\cdot r_0}$$

$$\frac{\delta c_v}{r_0^2} = \frac{\rho}{\lambda}\cdot\frac{Ea_Q}{RTw_C^2}\cdot Z_Q\cdot\exp(-Ea_Q/RTw_C)$$ Determination of Tw_C at given r_0

$$\frac{\delta c_v}{r_{0C}^2} = \frac{\rho}{\lambda}\cdot\frac{Ea_Q}{RTw^2}\cdot Z_Q\cdot\exp(-Ea_Q/RTw)$$ Determination of r_{0C} at given Tw

δc_c	FKP_C at constant surface temp. of self heating substance, shape dependent [-]
δc_v	FKPC at variable surface temp. of self heating substance, shape dependent [-]
r_0	characteristic length of the geometry of self heating substance
T_S	temperature at surface of self heating substance; if h = ∞ then T_S = Tw
V	volume of the geometry of self heating substance
S	surface of the geometry of self heating substance
e	Euler number, e=2.71828
h	heat transfer coefficient [energy/time/surface/K]
Nu	Nusselt number $Nu=2\cdot r_0\cdot h/\lambda$

Principle of Finite Elements (FE) solution of General Heat Balance Equation

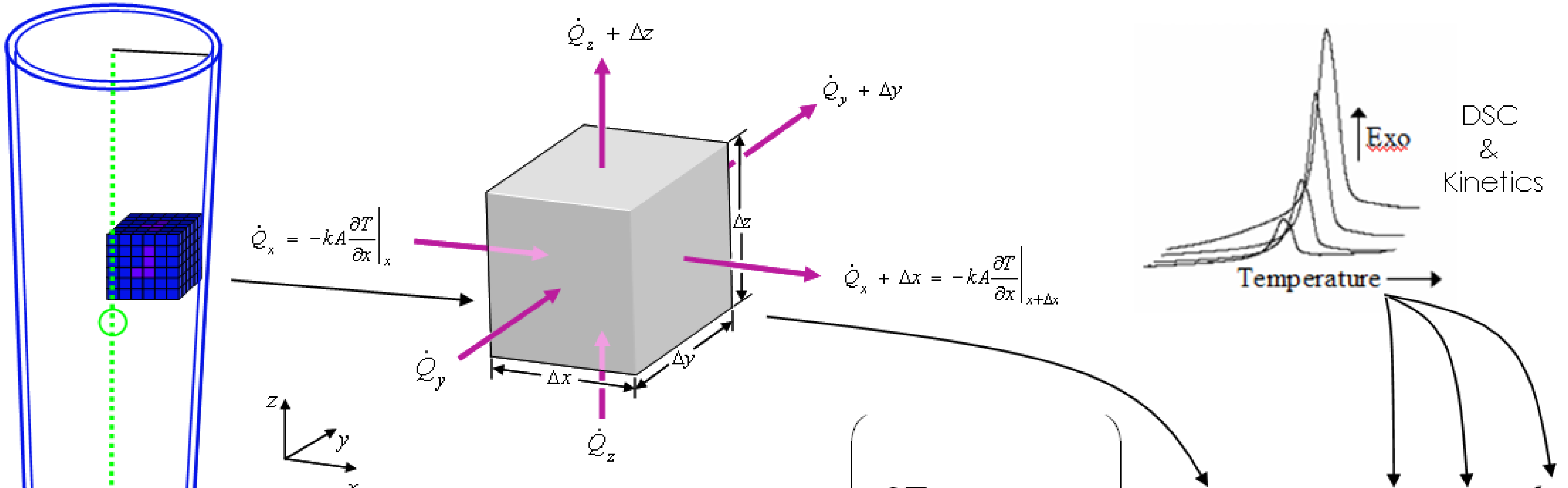

$$\rho_s\, c_{p,s}\left(\underbrace{\frac{\partial T_s}{\partial t}}_{\text{energy storage}} + \underbrace{\vec{u}_s \cdot \nabla T_s}_{\text{enthalpy convection}}\right) = \underbrace{\lambda_s \nabla^2 T_s}_{\text{heat conduction}} + \underbrace{\rho_s\, c_{p,s}\, \Delta T_{ad}\, \frac{d\alpha}{dt}}_{\text{Heat generation}}$$

Pre-requisites needed to perform the simulation

- Thermal decomposition behaviour, which is determined by DSC in closed, pressure resistant crucibles
  - for PUR foam PU8
  - for the propellant body
- Parameterization of the DSC measurements to be usable in the FE calculations
- Heat conductivity of the PUR foam (formulation PU8)
- Heat conductivity of the propellant body PB
- Specific heat capacity for PUR foam PU8
- Specific heat capacity for propellant body PB
- Mass density for PUR foam PU8
- Mass density for propellant body PB
- Heat conductivity, specific heat capacity, mass density for the steel of the burning chamber and of the air enclosed in the central bore of the PB
- Geometrical dimensions of the arrangement, rotational symmetry is given
- Heat transfer coefficient between outside air, acts here also as heat reservoir, and the steel body

Sample bodies to determine hat conductivity with the HotDisk™ method

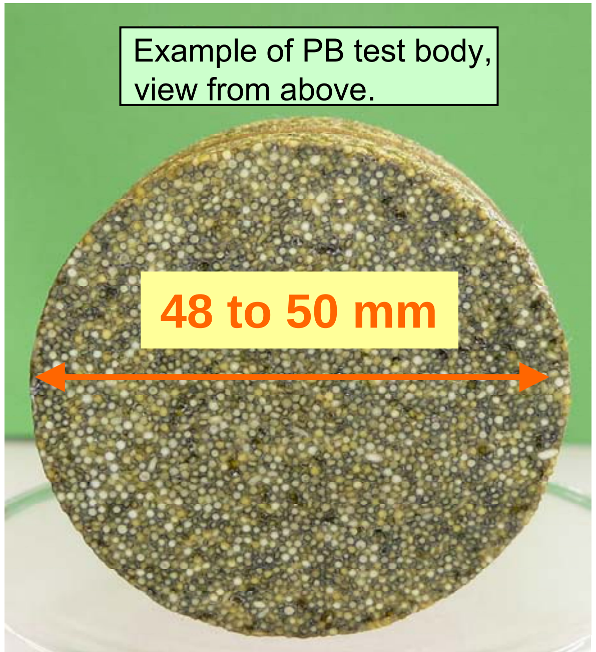

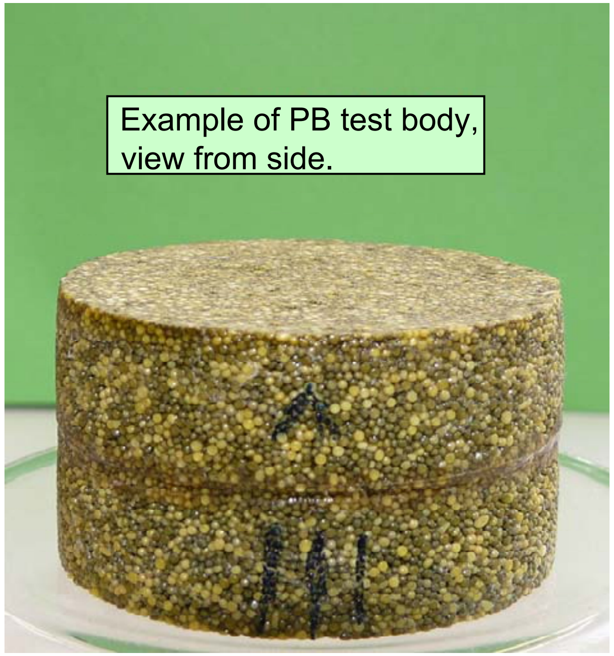

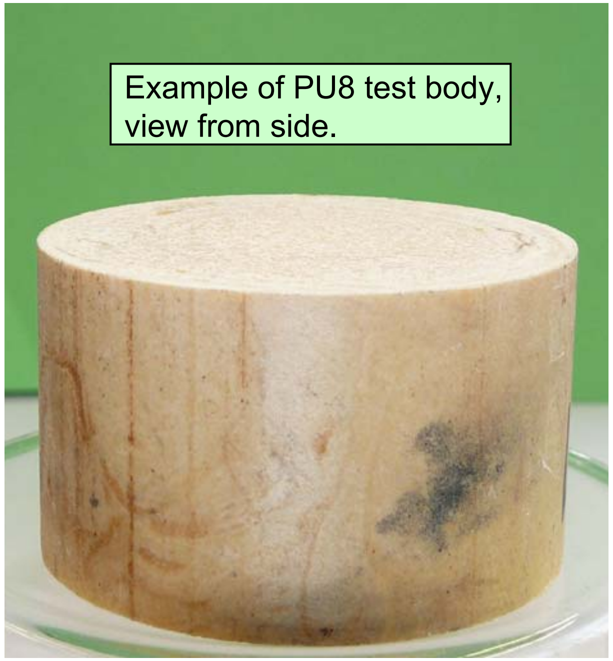

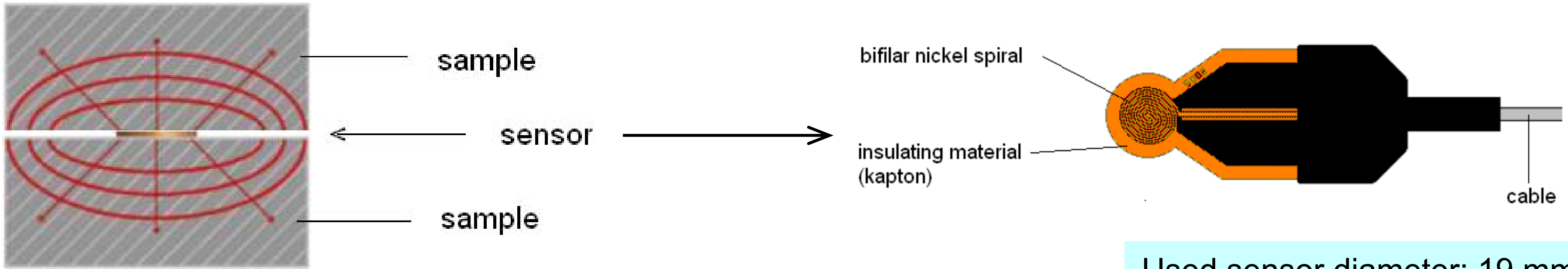

Used sensor diameter: 19 mm

Determined temperature rises for the two samples in HotDisk™ measurement

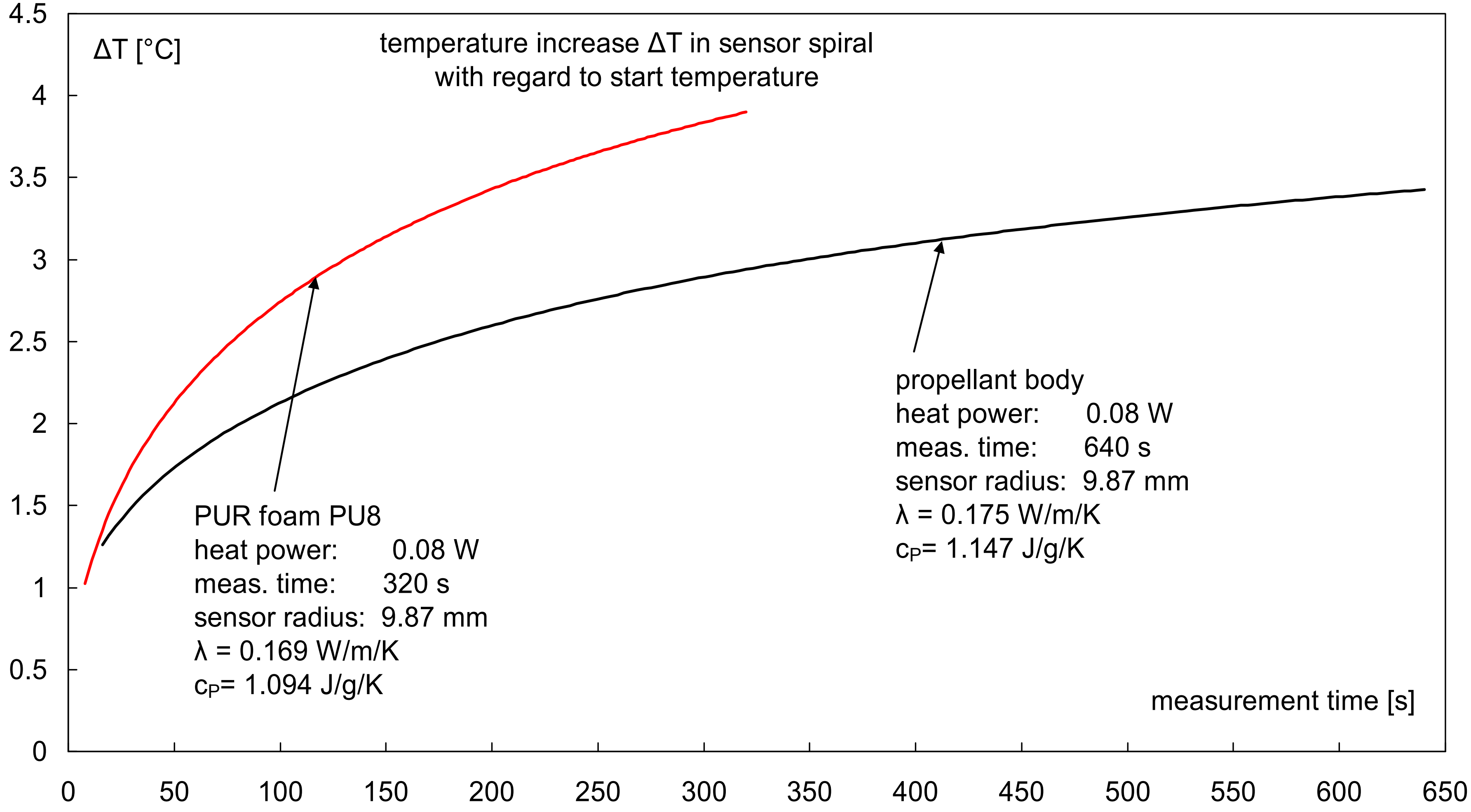

Fraunhofer ICT

DIEHL BGT Defence

Thermal data of polyurethane foam spacer

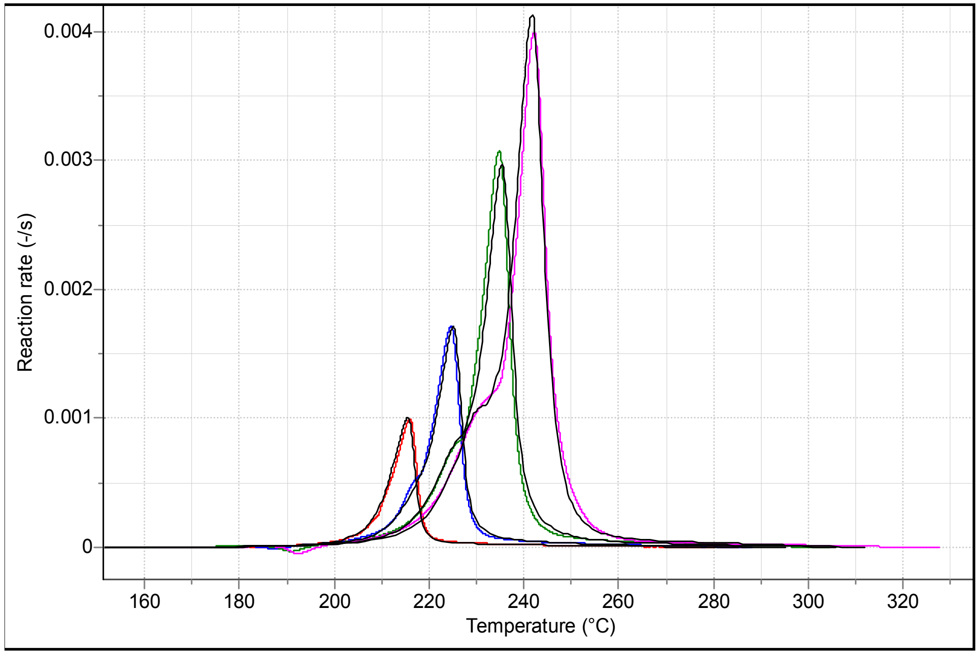

DSC data of the spacer foam PU8. Measured (coloured) and modelled (black) heat flow curves at the heating rates 0.5, 1, 2, 3 °C/min.

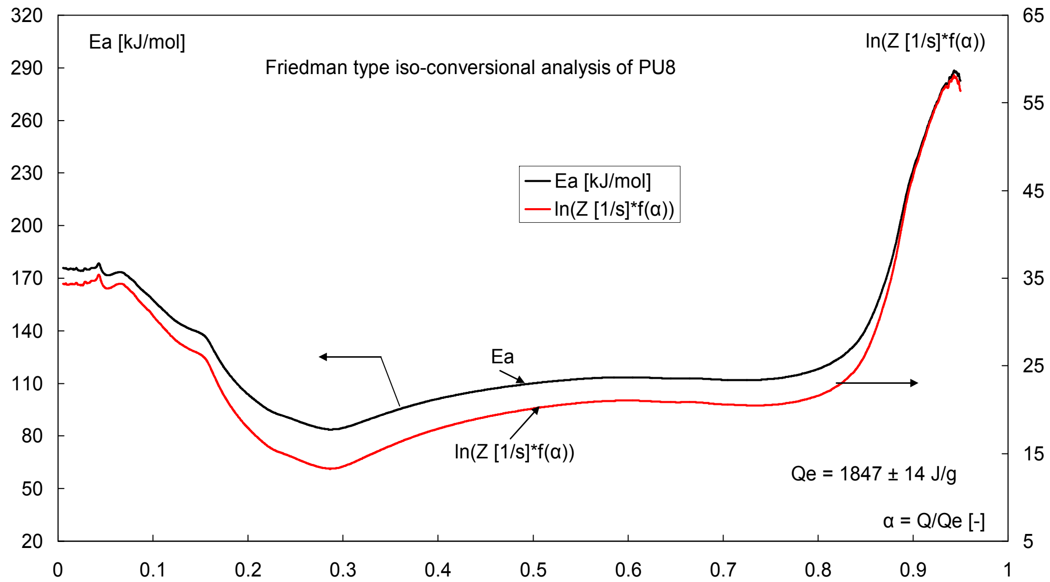

Result of the Friedman analysis (=differential iso-conversional data analysis) of the DSC data of the spacer foam PU8. Activation energy and pre-exponential factor as function of conversion of the exothermal decomposition reaction.

Thermal data of propellant body

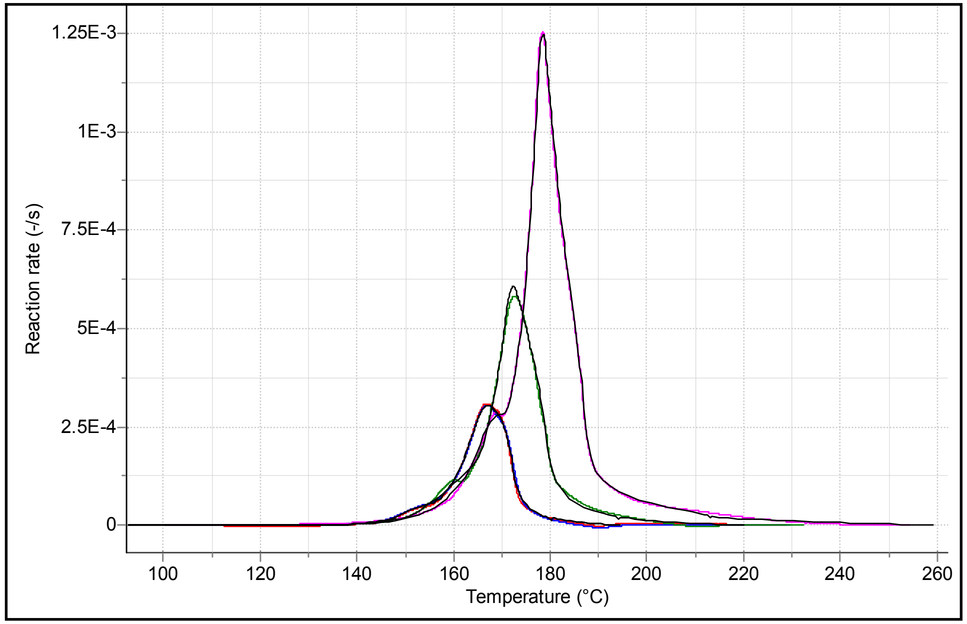

DSC data of the ball powder based propellant body. Measured (coloured) and modelled (black) heat flow curves at the heating rates 0.25, 0.5, 1 °C/min.

Result of the Friedman analysis (=differential iso-conversional data analysis) of the DSC data of the propellant body. Activation energy and pre-exponential factor as function of conversion of the exothermal decomposition reaction.

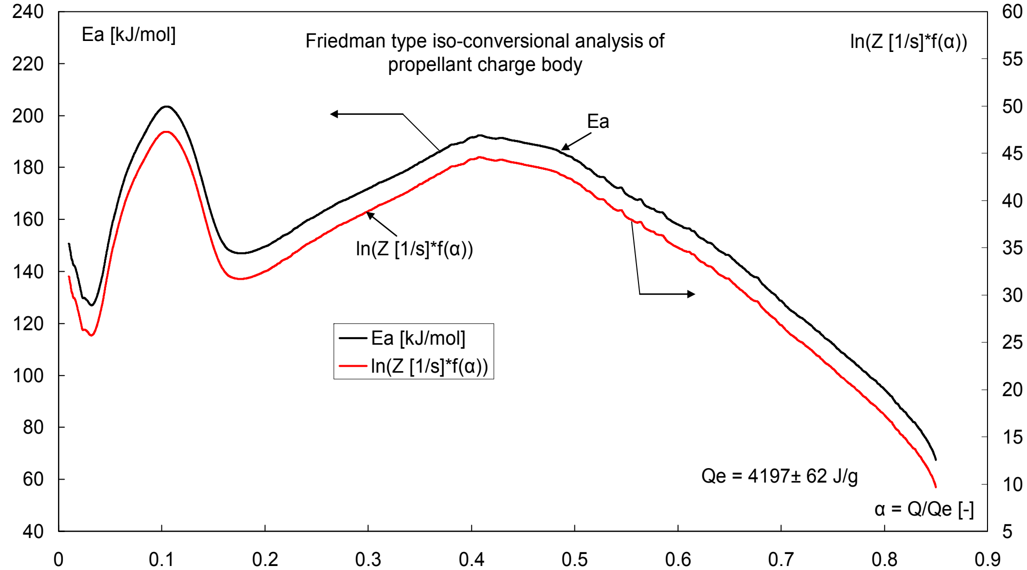

Layer scheme used in simulation

Layer scheme of the calculations with FE programme package.
Layer no. 2, 3 and 4 are energetic.
A cylindrical geometrical arrangement was used.

Layer material	Layer thickness [mm	Layer No.	Thermal decomposi-tion in layer	Initial temp. [°C]	Heat trans-fer number h [W/cm²/K]
Heat reservoir (air)		0	-	300	50
Steel	10	1	-	300	-
PU8 spacer	1.1	2	x	20	-
PU8 coating of PB	0.1	3	x	20	-
Propellant body (PB)	8.8	4	x	20	-
Central bore of PB	2.5	5	-	20	-

The AKTS software was used: the Thermokinetics and the Safety module

Layer sequence with temperature course after simulation run

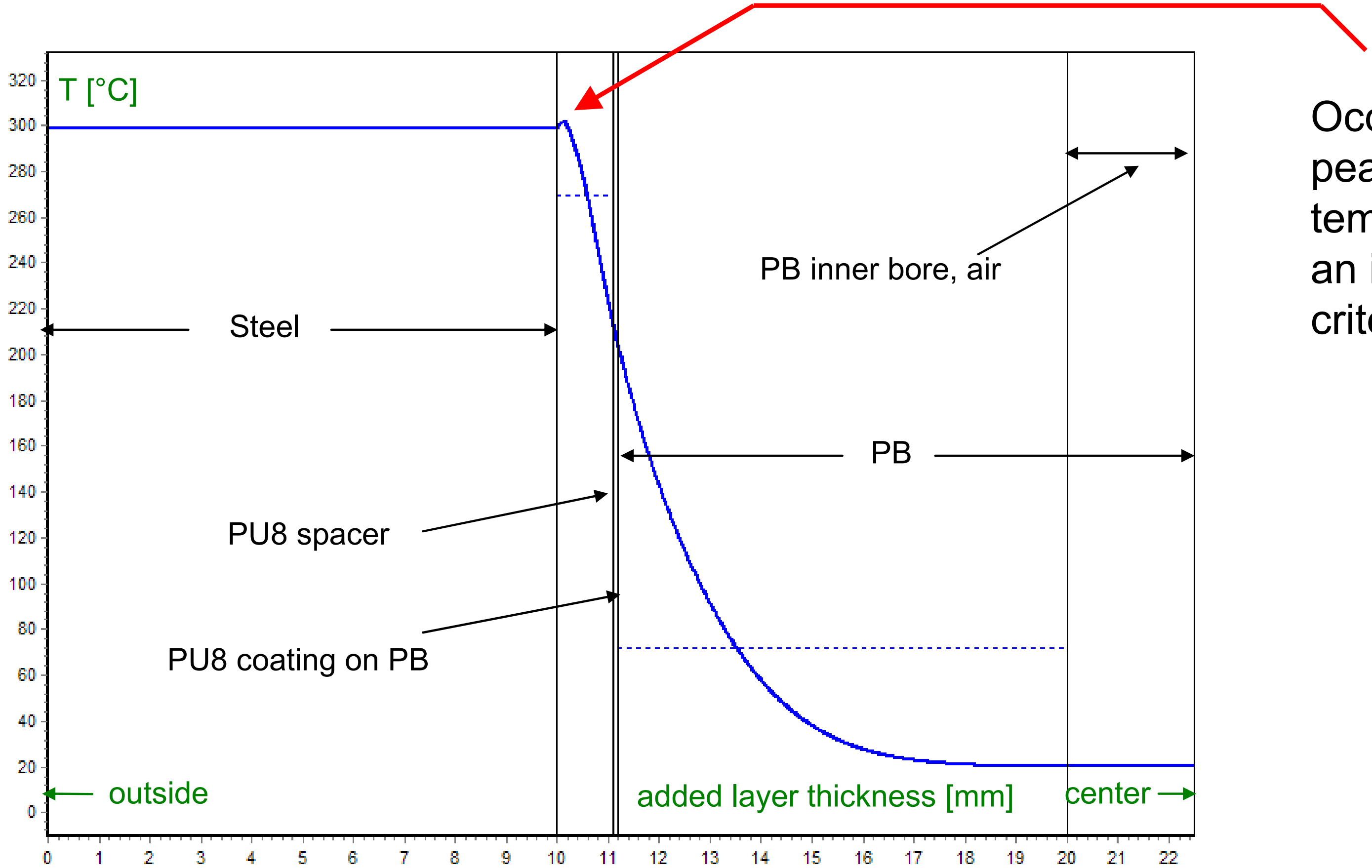

Occurrence of peak in rising temperature is an ignition criterion

Graphical presentation of the layer system used. Layer thicknesses are given in Table 7.
The diagram shows a calculation at 300°C.
To be noted is the starting peak of the temperature in layer 2, the PU8 spacer.

Temperature – time course in layer 1 and layer 2 at outside-T = 300°C

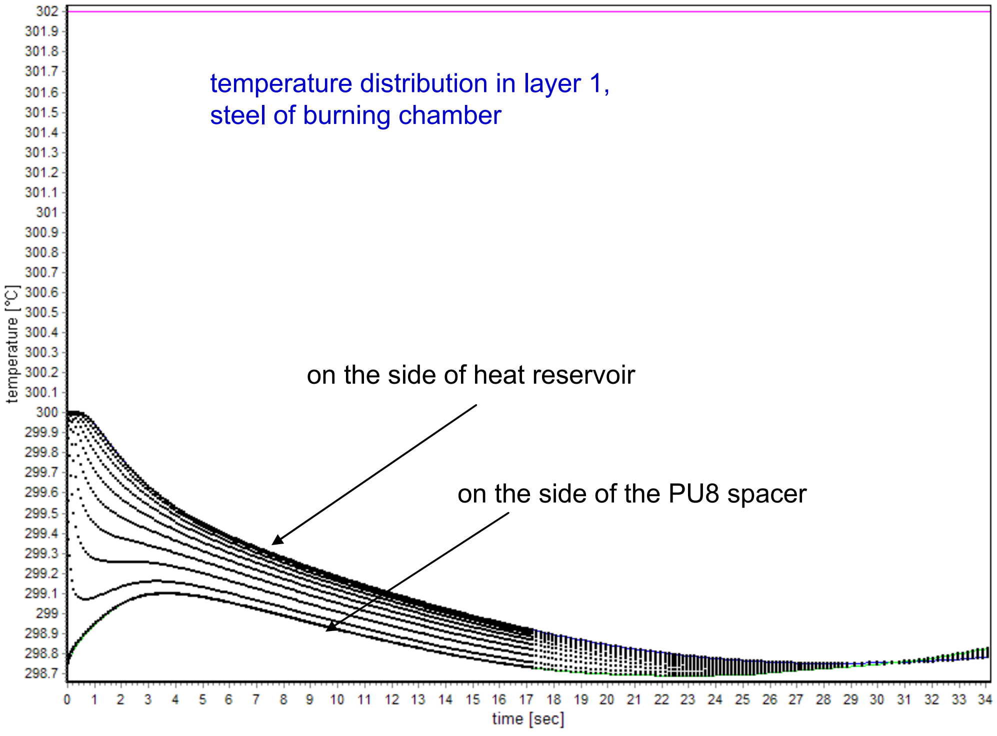

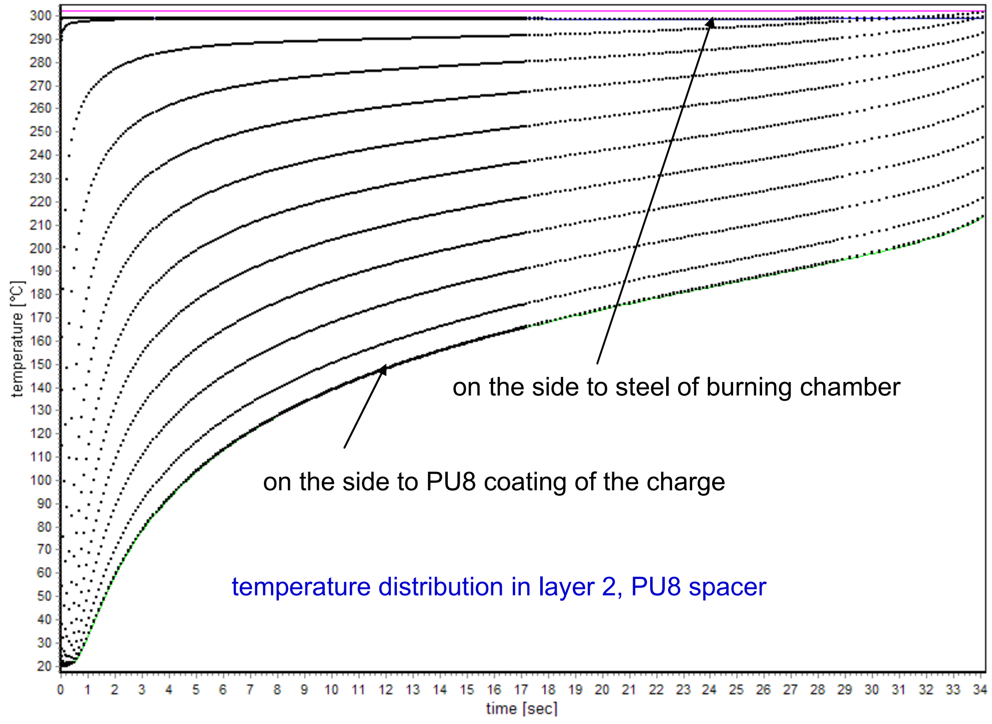

Temperature – time course in layer 3 and layer 4 at outside-T = 300°C

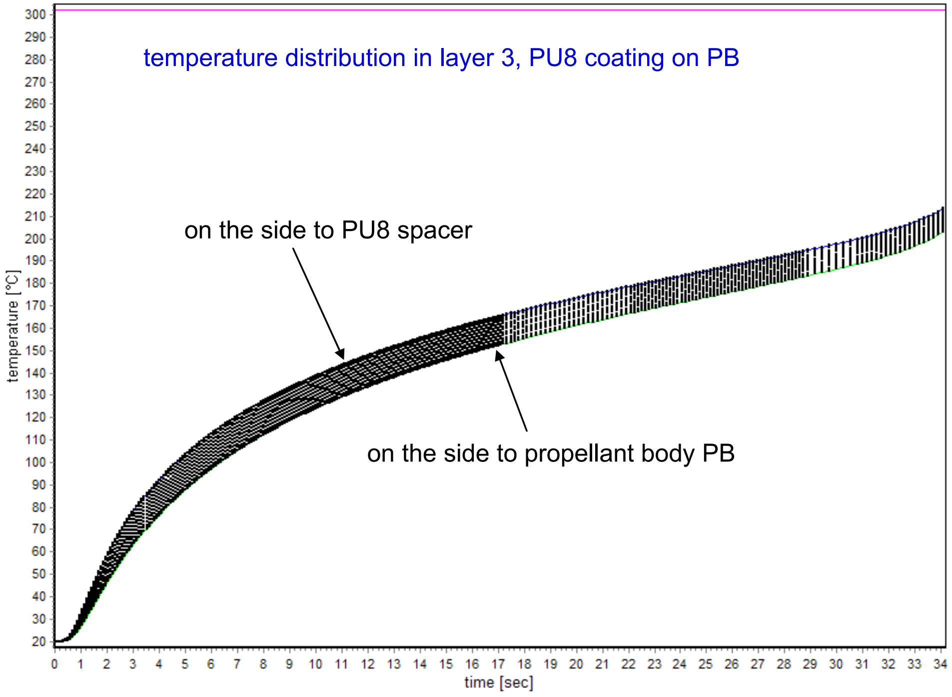

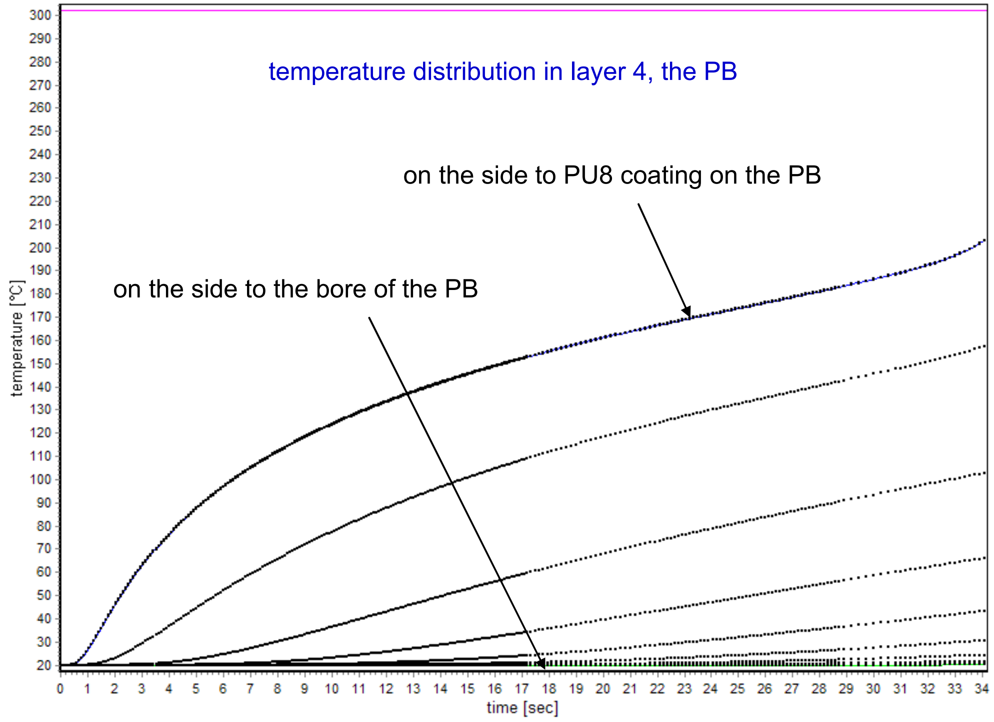

Criteria for the ignition of PU-foam and propellant body PB

Two criteria for ignition have been applied:

- the occurrence of the peak in the rising temperature in any layer
- the temperature reaches 190°C in the propellant body
- the temperature reaches 210°C in the foam

Calculated times to ignition of the propellant charge with PUR spacers

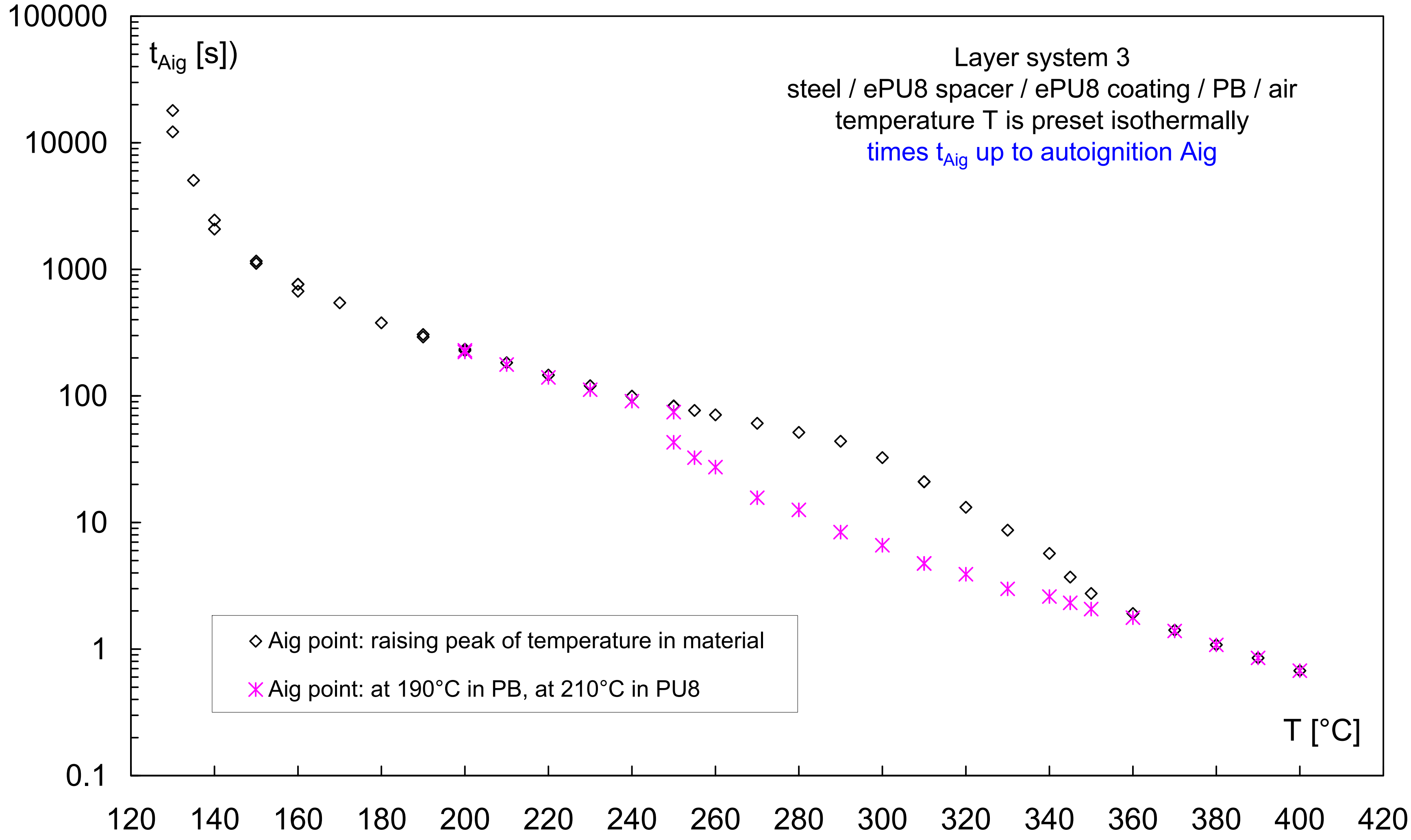

Comparison of calculated and measured time to ignition

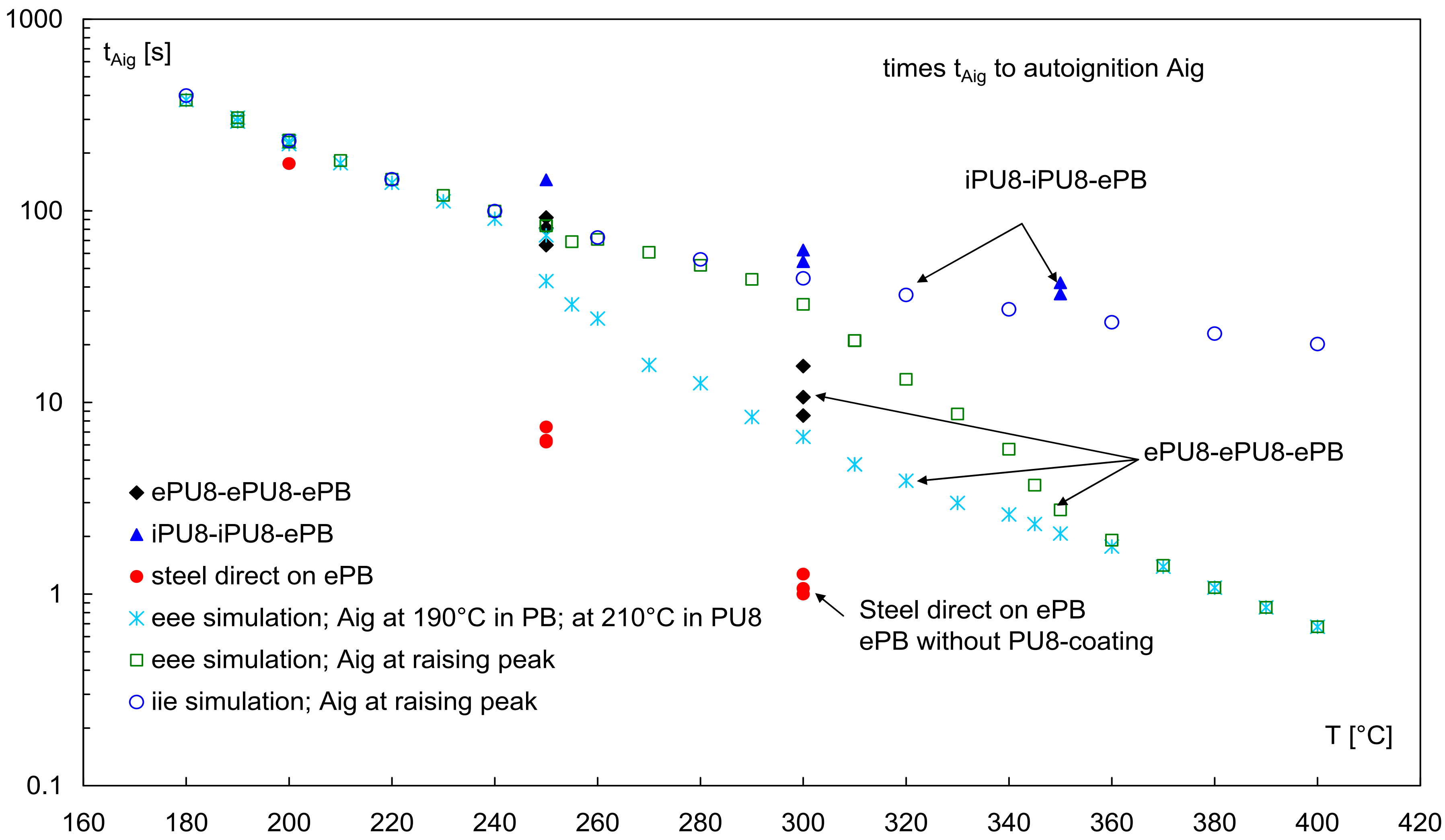

Arrhenius plot of times to autoignition t_{Aig} in the upper temperature range

All energetic.

Arrhenius plot of times to autoignition t_{Aig} in the upper temperature range,

The ignition starts in the energetic PU8 foam.

Ea = 143 kJ/mol

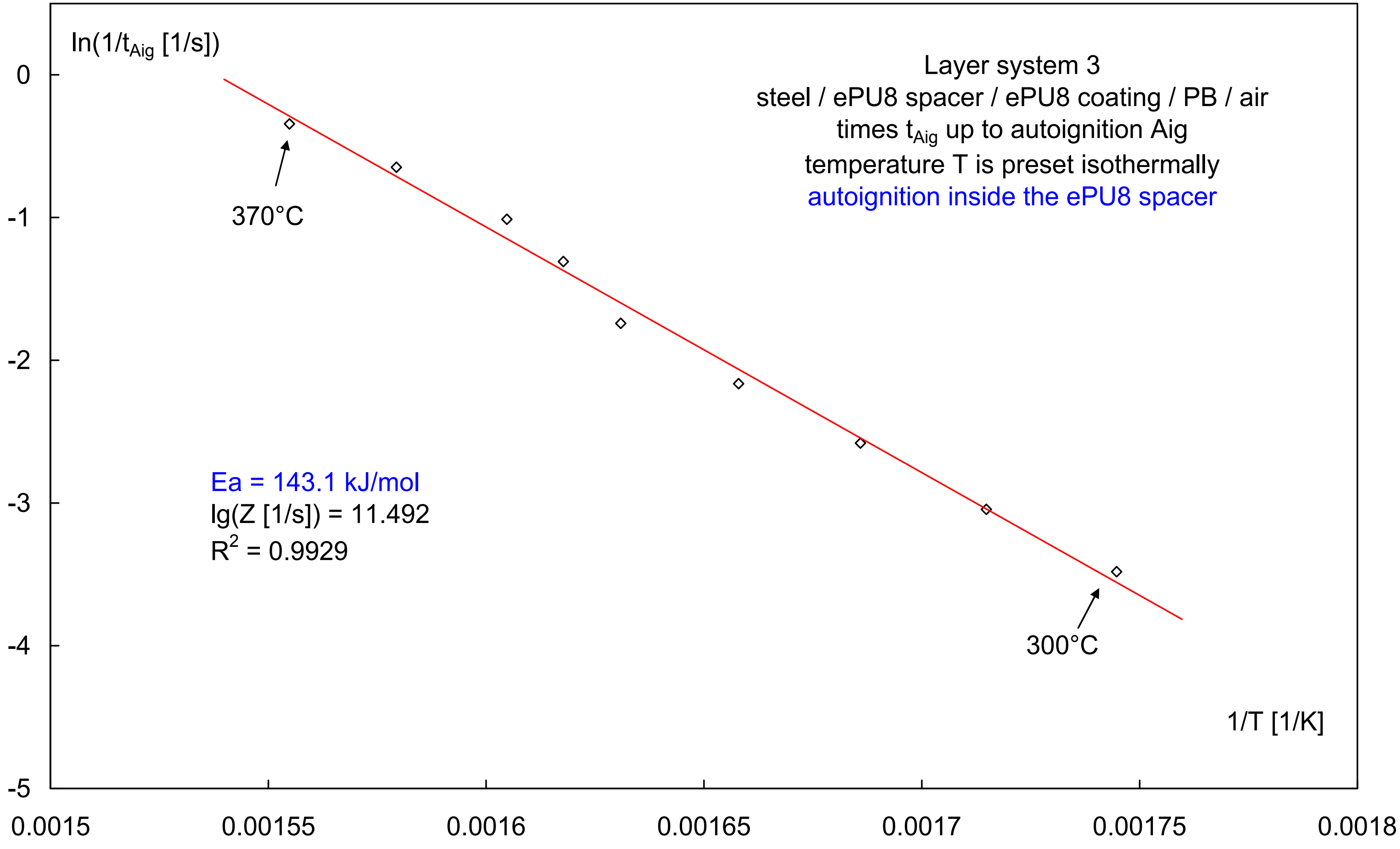

Arrhenius plot of times to autoignition t_{Aig} in the lower temperature range

All energetic.

Arrhenius plot of times to autoignition t_{Aig} in the lower temperature range.

The ignition starts in the NC-based PB.

The activation energy is remarkably low:

Ea = 41 kJ/mol

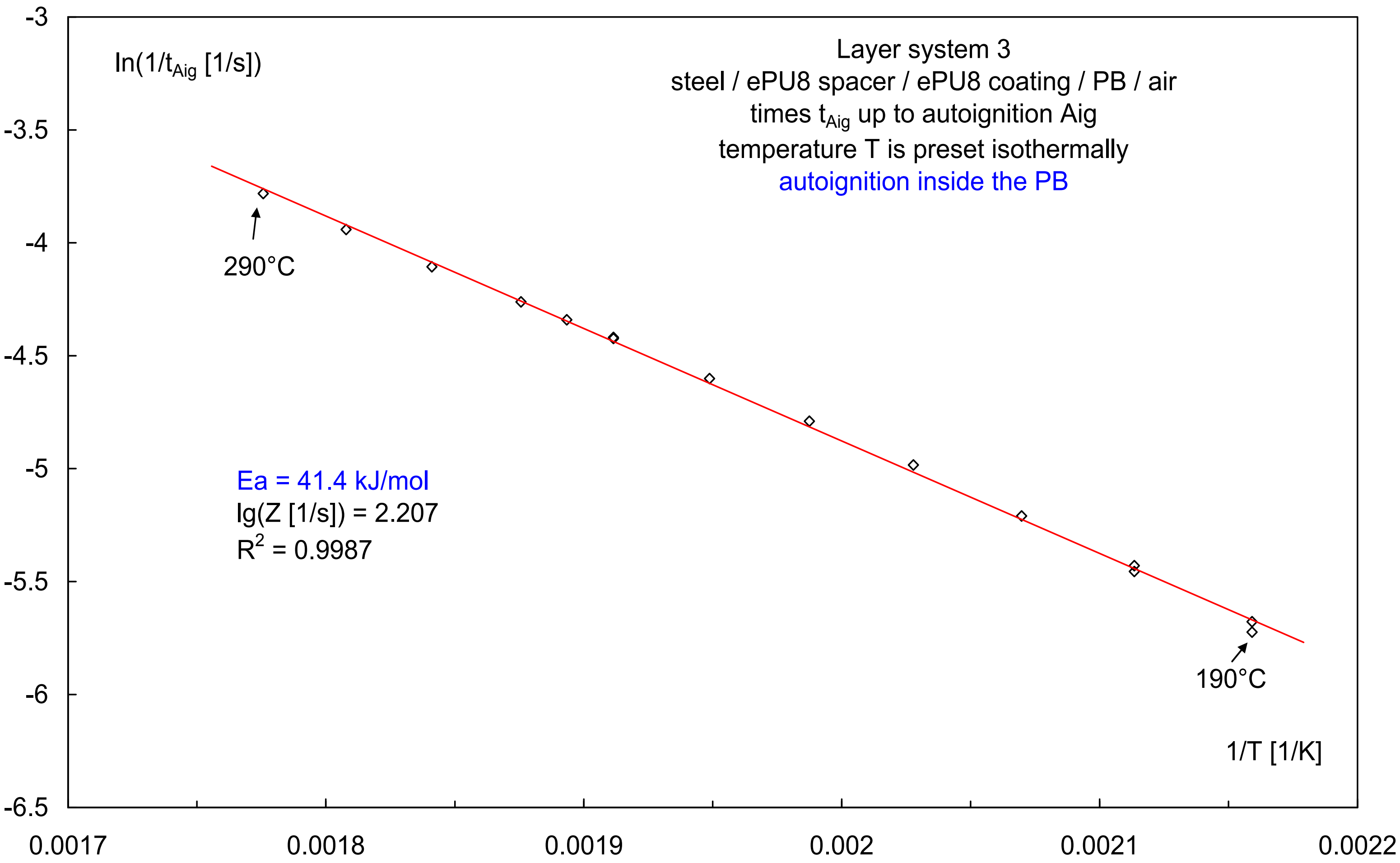

<u>Arrhenius plots of the times to autoignition t_{Aig}</u> -inert spacer and coating - energetic PB.

PU is inert

At high temperatures the activation energy is small indicating only a weak temperature dependence of t_{Aig}.

At low temperatures the activation energy becomes great, indicating long times t_{Aig} and strong temperature dependence.

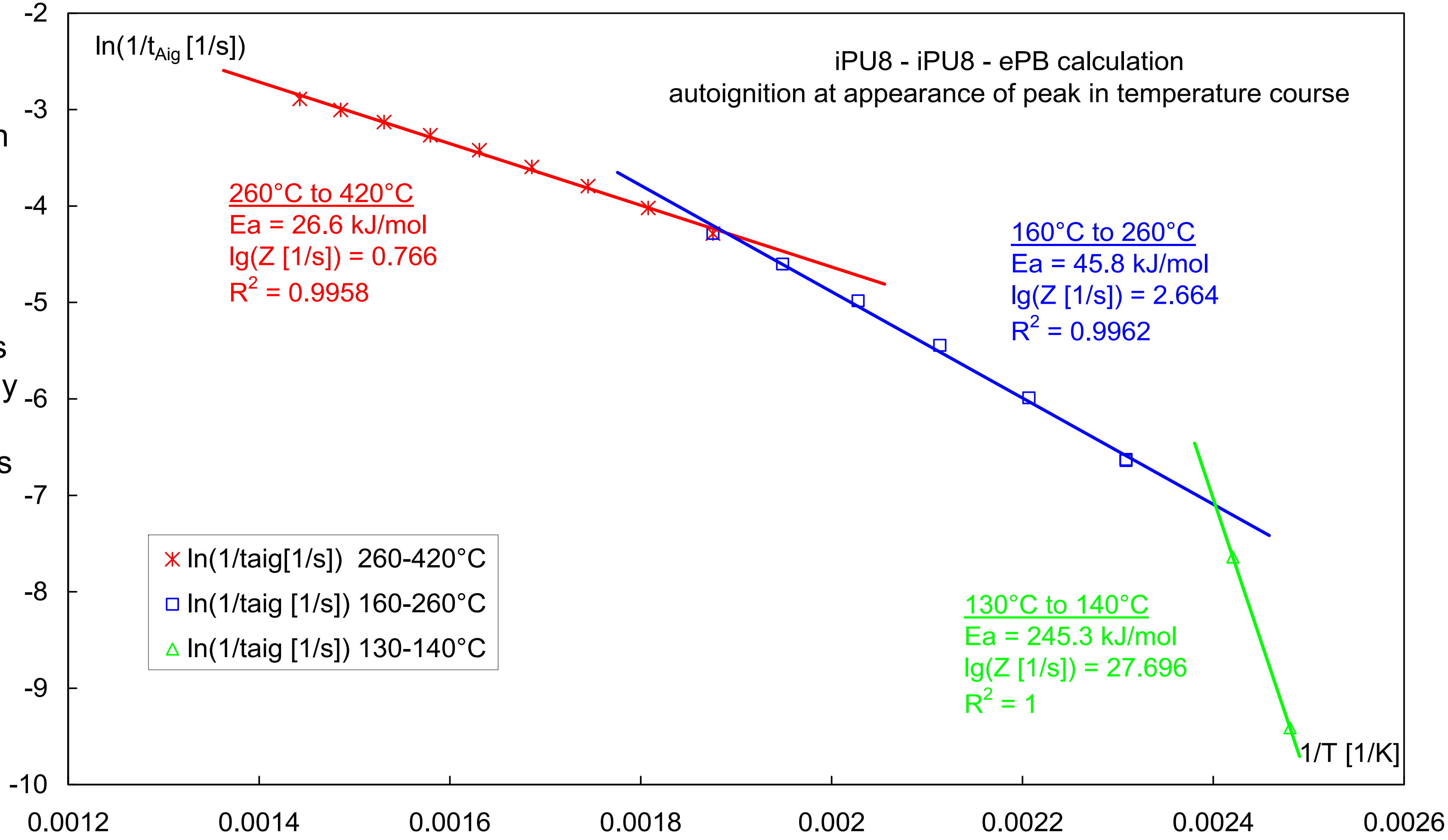

Fraunhofer ICT

DIEHL BGT Defence

Summary and conclusions

- Suitable foam was found by ICT to protect the caseless propellant body (PB)
- The foaming technology was developed by ICT
- ICT calculated the times to ignition of the foamed PB caused by hot burning chamber wall
- The thermal decomposition properties of PB and foam as well as heat conductivity and specific heat have been determined at ICT
- After the calculations company Diehl performed an experimental determination of the cook-off times of the propellant body
- The agreement between calculations and experimental determination is very good.

- In the temperature range 250°C to 350°C a bifurcation of the time to ignition occurs
  This effect may be seen as a type of 'ignition instability' of the material
  meant in the way that it has two possibilities to ignite – in foam or in PB
- This bifurcation is verified experimentally also by a greater scattering than outside this temperature range

Insert

Recourse to the 7th HFC-Symposium on Energetic Materials

Typical conversion-time-temperature graph with DSC and TGA

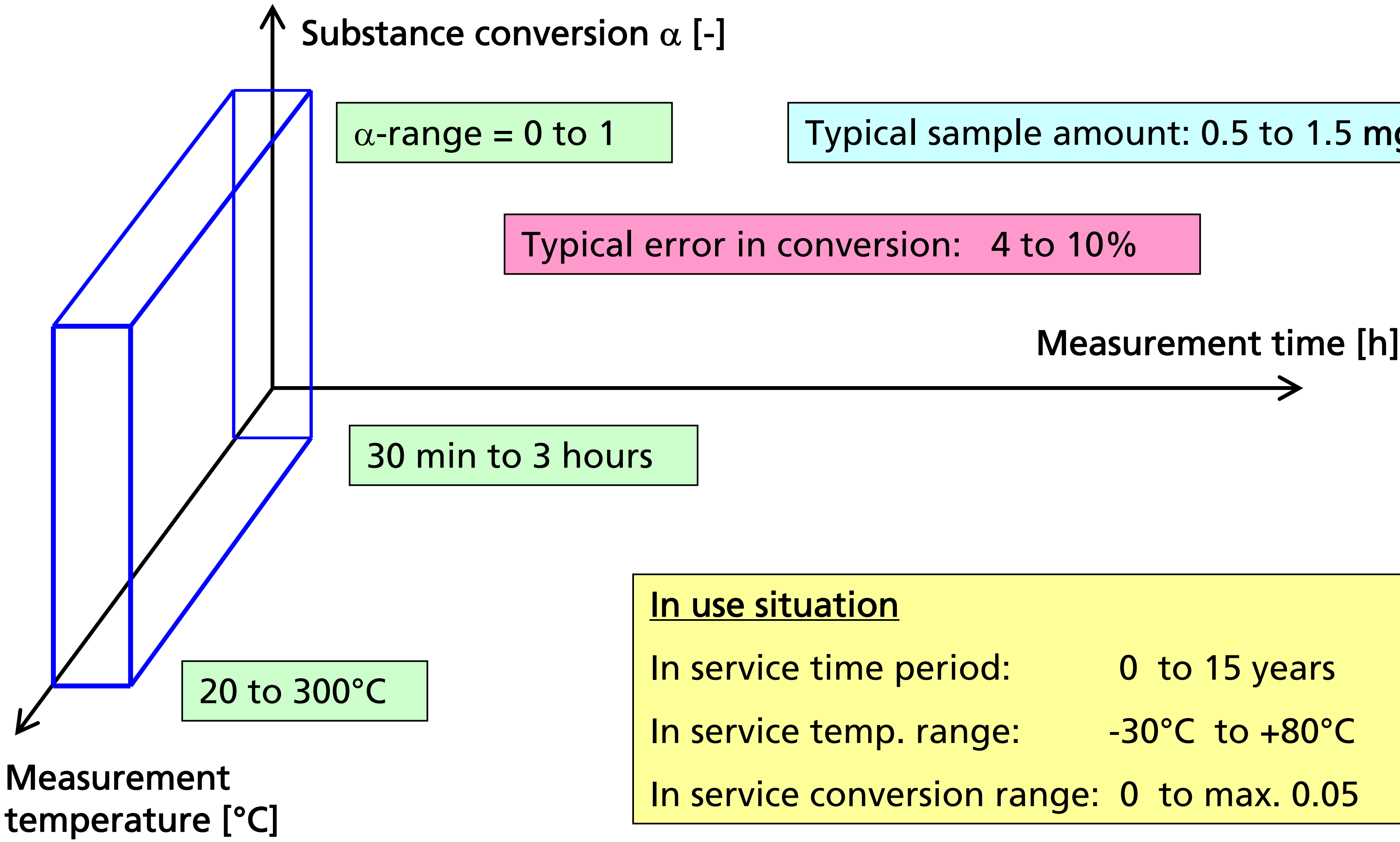

In use situation

In service time period: 0 to 15 years

In service temp. range: -30°C to +80°C

In service conversion range: 0 to max. 0.05

Fraunhofer ICT

Typical conversion-time-temperature graph with HFMC and ML(g amounts)

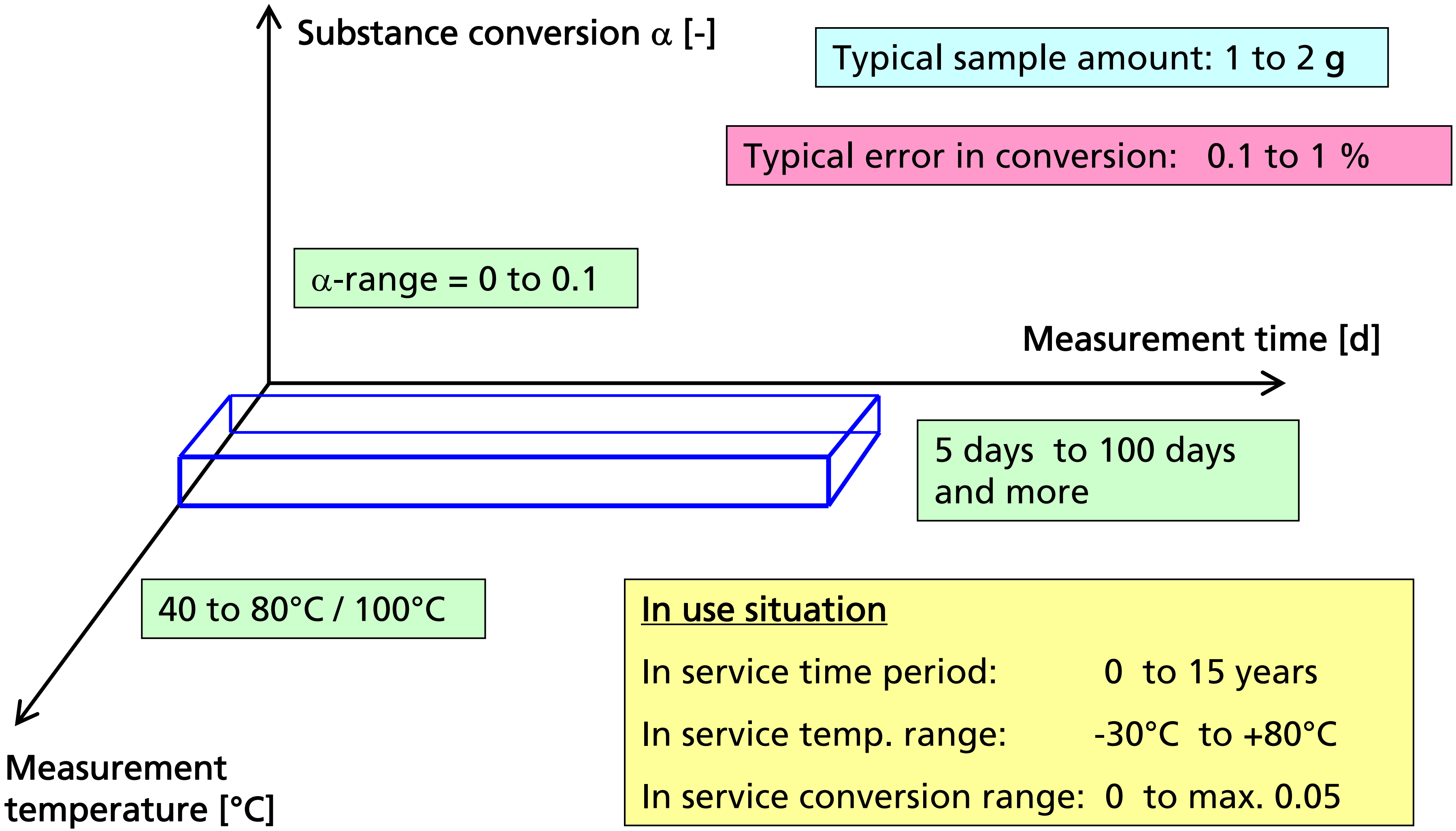

Fraunhofer ICT

Conclusion (from the 2010 presentation on 7th HFC-S on EM)

……

Sensitivity and speed in experimental data acquisition

To acquire data near the in-service temperatures needs time. The principle of equivalent load should be fulfilled.

Standard thermoanalytical equipment as DSC and TGA can provide with a set of experimental data in just one day.

But their accuracy is much lower than the one of the high sensitivity microcalorimeters. With DSC the error in reaction heat is often in the range or is even larger than the heat produced during full in-service time. This gives in prediction errors up to 200 % and more.

for the low temperature prediction !!

In contrast:

DSC data are suitable to predict high temperature processes.

Fraunhofer ICT

Acknowledgement

Company Diehl BGT Defence is thanked for financing the project and for the permission to present the results.

Thank you for your attention

Questions?